IEEE Access
Multidisciplinary | Rapid Review | Open Access Journal

Received August 22, 2019, accepted September 6, 2019, date of publication September 10, 2019, date of current version January 9, 2020.

Digital Object Identifier 10.1109/ACCESS.2019.2940480

The Estimation and Compensation of the Loop-Parameter-Drifting in the Digital Close-Loop Quartz Flexible Accelerometers

LONGJUN RAN[1], CHUNXI ZHANG[1], LAILIANG SONG[1], AND JIAZHEN LU[2]
[1]School of Instrumentation Science and Opto-electronics Engineering, Beihang University, Beijing 100191, China
[2]School of Aeronautics and Astronautics, Central South University, Changsha 410083, China

Corresponding author: Lailiang Song (songlailiang@gmail.com)

ABSTRACT There have been increasing demands for the long-term performance retention of the Quartz Flexible Accelerometers (QFA), extensively employed in the Inertial Navigation System (INS). Considering the convenience of conducting the parameter identification and control algorithm, the Digital Close-Loop QFA (Digital-QFA) is established to improve the long-term performance. Based on the model of the entire close-loop system, the interfering factors relating to time are analyzed in detail, both in the forward channel and the feedback channel. Two schedules are proposed to estimate the gain variation, utilizing the modulating signal and the feedback signal separately. According to the reference gain settings in ideal conditions, the forward and the feedback gain drifting of the system are calibrated online through the adjustment of the digital controller and the reference voltage of the DA-chip, separately. The simulation experiments show that about 90.26% of the gain-drifting could be estimated and about 87.56% of the output error of the accelerate could be restrained. Consequently, the proposed schedules could promote the long-term stability of the Digital-QFA significantly.

INDEX TERMS Digital close-loop quartz flexible accelerometers, drifting over time, estimation and compensation, long-term performance, loop-parameters.

I. INTRODUCTION

The Accelerometer is the primary component of Inertial Navigation System (INS), and it could provide the non-gravitational acceleration of the carrier relating to inertial space [1]. There are series accelerometers with different assembly processes, including Electrostatic accelerometer, Floated pendulous accelerometer, Quartz Flexible Accelerometer (QFA), MEMS Accelerometer, etc. They do have different accuracy indexes and application fields, and the typical characteristics of these accelerometers are stated in TABLE 1 [2]. The core problems of the accelerometer contain the improvement of the performance of its static accuracy (Resolution, Bias and Scale factor, etc.), dynamic characteristics (Range, Bandwidth, Vibration Rectification Error, etc.), etc. And there did pay much attention to the improvement of the accuracy of measurement. Different signal detection structures and temperature compensation were executed to improve the accuracy and achieve better temperature performance [3]–[5]. The detection error of the accelerometers resulting from vibrations or other dynamic environment was analyzed in detail. Simulation optimization approaches and several process constraints were proposed to improve the dynamic performance [6].

For the Navigation-level applications of accelerometers, the QFA is the most appropriate one considering the cost, size and weight, etc. With the extensive application in the Chariot, Warship, Aircraft, the QFA, satisfying the Navigation-level applications in INS, does start its high-speed development and the key problems tackling.

The Analog Close-Loop QFA (Analog-QFA) is extensively applied in the inertial field, and QA-series accelerometers from Honeywell are the typical high-performance products [7], [8]. The application of Analog-QFA does have its limitations attributing to the additional analog-to-digital conversion module when integrated in INS, which would increase the uncertainty of measurement. Benefiting from the

The associate editor coordinating the review of this manuscript and approving it for publication was Fabio Massaro.

TABLE 1. The typical characteristics of series accelerometers.

	ELECTROSTATIC ACCELEROMETER	FLOATED PENDULOUS ACCELEROMETER	QFA	MEMS
Bias Stability	0.1-1ug	1-10ug	5-100ug	100-1000ug
Scale Factor Stability	1-10ppm	10ppm	10-100ppm	100-1000ppm
Cost	Most	High	Medium	Lowest
Manufacturing cycle	Thousands of hours	Thousands of hours	hundreds of hours	Dozens of hours

development of digital chips and digital MEMS accelerometers [9]–[12], there developed Digital Close-Loop QFA (Digital-QFA) scheme as certain direction of exploration to improve its dynamic performance, and the Digital-QFA could also provide new ways to measure the inner parameters of the whole-loop.

There were series researches about the model of Analog-QFA to improve its performance and scale production capacity [13]–[15]. The Digital-QFA does have the same inner structure: Differential Capacitance, Electromagnetic Torque Feedback, etc. Whereas the difference is the signal detection and processing schedule. Applying embedded chip, there would be multiple detection methods of differential capacitance; for instance, Switched Capacitor Detection Method, Modulation/ Demodulation scheme [16]–[19], etc. And the Modulation/ Demodulation scheme based on AC-bridge is the most promising approach for micro capacitance measurement, which is extensively employed in Accelerometers, Capacitance tomography system [20]–[22], etc. Additionally, modern control theory could be employed in the digital system to improve its dynamic performance [23]. And the multiple control algorithms would provide new parameter identification methods to establish more accurate models [24], [25].

The long-term stability is also the core index of the accelerometers, which could be included in the static accuracy, and it has significant impact on the performance maintenance in storage period of most Weapons. The long-term stability of both Analog-QFA and Digital-QFA is still the weak indicator in INS. The drifting of the Bias and the Scale-factor of the accelerometers would reach 100 ug and 100ppm in one year [7], and the degradation of the performance should attribute to the loop parameters of the QFA be varying over time. The variation of loop parameters, as amplifier characteristics, resistors, structural changes, would bring about the gain of the close-loop be drifting. And it could lead to the deterioration of the controller and the drifting of the scale factor. The estimation and compensation of the loop-gain variation become significant works to improve the long-term performance of the accelerometers. There are several approaches to estimate the gain variation in Digital Close-loop systems [23], [26], [27], which is the significant advantages of Digital-QFA over Analog-QFA.

For the application of the accelerometer itself, the parameters (Bias, Scale factor, cross coupling factors, etc.) could be calibrated through several different known rotations [28], [29]. For the currently application of the accelerometers in the INS, the parameters should be calibrated through the High-Precision-Turntable. With the condition of long-time on service, the entire system must be disassembled from the carriers (weapons, vehicles, aircrafts, etc.) to re-calibrate the critical parameters precisely at fixed intervals, when there is not any external reference information [30], [31]. And it should be great consumption of manpower and material resources. For the application of accelerometer, the self-detection or self-estimation approaches without the turntable at sensors-level are lack of research. These new methods would improve the efficiency of calibration and provide new ways to judge the loop-parameter drifting. The estimation and compensation schedule in this paper is motivated by these factors, and it might be a new avenue to support the sensor-level-self-detection in the INS application. The main contributions of this paper are summarized as follows:

1) More perfect mathematical model is established for the Digital-QFA and most of the influence factors varying over time are analyzed detailly.
2) The forward-gain is estimated in the open-loop status and the modulation signal and the working characteristics of the Digital-QFA are fully considered. About 90.26% of the forward-gain drifting is estimated and compensated effectively.
3) Considering the inaccurate measurement when the Digital-QFA work in open-loop state, the constant current reference is introduced to the estimation schedule. About 90.92% of the feedback-gain drifting is estimated and compensated effectively.
4) The forward-gain drifting is compensated in the PID controller, and the feedback-gain drifting is compensated through adjusting the reference voltage of the DA chip in the feedback channel.

The drifting of the parameters of the close-loop system would bring about two principal problems: the stability problem of the control system, and the output-drifting of the sensor.

A. STABILITY PROBLEM OF THE CONTROL SYSTEM

The optimization of the control algorism would aim to improve the anti-interference performance, or the stability of the system. The parameters of structure, circuits, and

the materials would vary when the surrounding environment changing. The perturbation range of these parameters should be analyzed first, and the System Sensitivity Function would be the design philosophy of the control system. The Anti-jamming ability, Gain margin, and the Phase margin would be the judgement-criterion of the effectiveness of the algorism.

B. OUTPUT-DRIFTING OF THE SENSOR

Core issues of this paper. The output-drifting of the sensor, more emphasizing on static characteristic preservation, would be the core point and self-detection or self-calibration is the key innovation.

The rest of this paper is organized as follows. In Chapter II, the entire model of the Digital-QFA would be represented. The mechanism of the entire loop-parameters changing would be analyzed, and the final presentation of the gain variation is descripted in detail. The estimation and compensation of the forward gain and the feedback gain variation are represented in Chapter III. The experiment verification and discussion are stated in Chapter IV. Finally, the summarize of this paper and the possible future researches are concluded in Chapter V.

II. THE LOOP-MODEL AND THE PARAMETER-VARIATION OF DIGITAL CLOSE-LOOP QFA

The Digital-QFA is composed of sense organ, signal detection and feedback circuit, electromagnetic torque. The sense organ is a flexible pendulum, shown in Fig. 1, which deviates away from the equilibrium position when sensing the external acceleration.

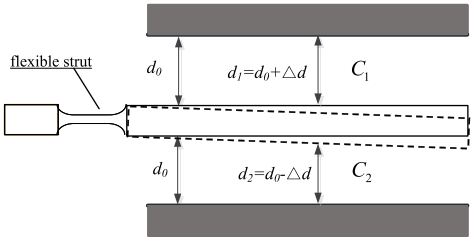

FIGURE 1. The sense organ of the accelerometer.

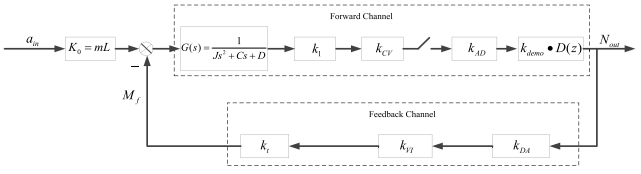

FIGURE 2. The Loop-Model of the Digital Close-Loop QFA.

The model of the QFA had been researched in many articles [14], [32], and the loop model of the Digital Close-Loop QFA in this paper is shown in Fig. 2. The entire loop is divided into three sections: ① pendulosity ($k_0 = mL$); ② forward channel; ③ feedback channel.

A. PENDULOSITY

The pendulosity is composed of the mass and the arm. On account of the sealing characteristics of the sense organ of the accelerometer, the mass of the pendulum could be assumed to maintain constant. The arm is affected by the linear expansion coefficient of the quartz material. Considering the smaller linear expansion coefficient and the mutual compensation of the accelerate torque and the feedback electromagnetism torque, it is rational to assume the pendulosity maintains constant.

B. FORWARD CHANNEL

The forward transfer function, $G(s) \cdot k_1 k_{CV} k_{AD} \cdot k_{demo} D(z)$, is composed of signal detecting and digital controller. Considering the demodulation module and the controller module are constant in the embedded chip, there would analysis the interfering factor of $G(s) \cdot k_1 k_{CV} k_{AD}$.

1) THE FIRST MODULE: $G(s) = \frac{1}{Js^2+Cs+D}$ [14], [32]

The deflection of the pendulum in steady-state could be computed as equation (1).

$$\begin{aligned}\theta &= \frac{M}{s} \cdot \frac{1}{Js^2 + Cs + D} \\ &= \frac{M}{s} \cdot \frac{1}{|s_2| - |s_1|} \cdot \left(\frac{1}{s + |s_1|} - \frac{1}{s + |s_2|}\right)\end{aligned} \tag{1}$$

where $s_{1,2} = \frac{-C \pm \sqrt{C^2 - 4DJ}}{2J}$. The function of the deflection over time is as follows.

$$\theta = M \cdot \frac{1}{|s_2| - |s_1|} \cdot \left\{ \frac{1}{|s_1|} \cdot (1 - e^{-|s_1|t}) - \frac{1}{|s_2|} \cdot (1 - e^{-|s_2|t}) \right\} \tag{2}$$

When $t \to \infty$, it can be simplified as:

$$\theta = M \cdot \frac{1}{|s_2| \cdot |s_1|} = M \cdot \frac{1}{D} \tag{3}$$

Therefore, the output deflection is only related to bending stiffness (D) at steady-state, when the input moment maintains constant. Considering that the bending stiffness is mainly determined by the elastic modulus of materials, and the elastic modulus of quartz would change little over time. And the little variation of elastic modulus can be further reduced through improvement of material and stressless processing technology. Consequently, it has little effect on the gain variation of the forward channel.

2) THE SECOND MODULE: $k_1 = 2C_0 \frac{L}{d}$ [14], [32]

This module is the function of arm, unilateral capacitance and plate spacing. It is mostly impacted by the coefficient of linear expansion of the quartz and it does change over time with great possibility. There assumes that the actual expression of the module as $\hat{k}_1 = k_1 \cdot (1 + \delta k_1)$.

3) THE THIRD MODULE: k_{CV}

Depending on the high precision reference capacitance, there employed AC-Bridge to measure ΔC. The scheme block diagram is exhibited in Fig. 3.

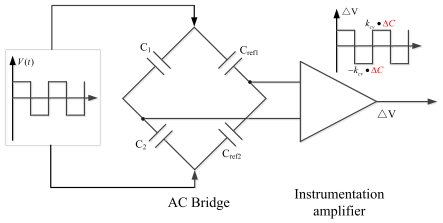

FIGURE 3. The Measuring scheme of ΔC depending on AC Bridge.

Suppose the amplification of the instrumentation amplifier is k_{amp}, and the modulation signal is V_{IN} , then it can be concluded:

$$\begin{aligned}\Delta V &= (\frac{C_1}{C_1+C_2} - \frac{C_{ref\,1}}{C_{ref\,1}+C_{ref\,2}}) \cdot V_{IN} \cdot k_{amp} \cdot \Delta C \\ &= k_{CV} \cdot \Delta C \end{aligned} \tag{4}$$

The reference capacitances are selected to compose AC bridge, and they must meet the conditions of $C_{ref\,1} = C_{ref\,2} = C_0$. The actual reference capacitances are signed as $C_{ref\,1}, C_{ref\,2}$, considering the parasitic capacitance, input capacitance of the instrument amplifier, etc. When the accelerometer is in steady-state, there can be conducted $C_1 = C_2 = C_0$. Then there can be obtained:

$$\frac{C_1}{C_1+C_2} - \frac{C_{ref\,1}}{C_{ref\,1}+C_{ref\,2}} = \frac{1}{2} - \frac{C_{ref\,1}}{C_{ref\,1}+C_{ref\,2}} \tag{5}$$

The absolute value of ΔC_{ref} does just have impact on the resolution of the differential capacitance, instead of the transfer gain. The variation of $C_{ref\,1}$ or $C_{ref\,2}$ over time (name as δC_{ref}) would have influence on the gain of CV converter, with minor value of δC_{ref}. There assumes that the actual expression of the module as $\hat{k}_{briege\_0} = k_{briege\_0} \cdot (1 + f(\frac{C_{ref\,1}}{C_{ref\,1}+C_{ref\,2}}))$, where $f(\frac{C_{ref\,1}}{C_{ref\,1}+C_{ref\,2}})$ is the function of the variation of $(C_{ref\,1}, C_{ref\,2})$.

$V_{IN}(\max) = N_{FPGA} \cdot \frac{V_{DA1\_ref}}{2^{N_{DA1}-1}} \cdot k_{tz}$ is the amplitude of the modulation signal. Where N_{FPGA} is the digital value produced by FPGA and it is constant over time; V_{DA1_ref} is the reference voltage of the modulation DA-chip, and it would vary over time as $\hat{V}_{DA1\_ref} = V_{DA1\_ref} \cdot (1 + \delta V_{DA1\_ref})$; k_{tz} is the magnification of the follow-up amplifier, and it is the function of resistance, characteristic of amplifier, etc. Therefore, the actual magnification can be calculated as $\hat{k}_{tz} = k_{tz} \cdot (1 + \delta k_{tz})$.

Similarly, k_{amp} is the magnification of amplifier and it could be computed as $\hat{k}_{amp} = k_{amp} \cdot (1 + \delta k_{amp})$.

In summary, the gain of CV converter is as follows.

$$\begin{aligned}\hat{k}_{CV} &= k_{CV}(1 + \delta k_{CV}) \\ &= k_{briege\_0} \cdot (1 + f(\frac{C_{ref\,1}}{C_{ref\,1}+C_{ref\,2}})) \\ &\quad \cdot N_{FPGA} \frac{V_{DA1\_ref}(1 + \delta V_{DA1\_ref})}{2^{N_{DA1}-1}} \\ &\quad \cdot k_{tz}(1 + \delta k_{tz}) \cdot k_{amp}(1 + \delta k_{amp}) \end{aligned} \tag{6}$$

4) THE FOURTH MODULE: k_{AD}

Considering the interference factors of AD, the actual gain of the module is stated in equation (7). Where N_{AD} is the digits of AD; $\hat{V}_{AD\_ref} = V_{AD\_ref} \cdot (1 + \delta V_{AD\_ref})$ is the reference voltage of AD, and it is also changing over time.

$$\begin{aligned}\hat{k}_{AD} &= \frac{2^{N_{AD}-1}}{V_{AD\_ref} \cdot (1 + \delta V_{AD\_ref})} \\ &\approx \frac{2^{N_{AD}-1}}{V_{AD\_ref}} \cdot (1 - \delta V_{AD\_ref}) \\ &= k_{AD} \cdot (1 - \delta V_{AD\_ref}) \end{aligned} \tag{7}$$

In summary, the influence factors of the gain of the forward channel conclude the reference capacitance, operational amplifier, resistance, AD, DA, etc. The overall gain of the forward channel would be diverse when the close-loop system be started at different condition, and it would affect the performance of the control system. There can be conducted that the gain variation is approximately presented as linear relation, as stated in equation (8).

$$\begin{aligned}\hat{k}_{pre} &= k_{pre} \cdot (1 + \delta k_{pre}) \\ &= \frac{1}{D} \cdot k_{demo} k(D(z)) \cdot k_1(1 + \delta k_1) \cdot k_{CV}(1 + \delta k_{CV}) \\ &\quad \cdot k_{AD}(1 - \delta V_{AD\_ref}) \end{aligned} \tag{8}$$

C. FEEDBACK CHANNEL

The gain of feedback channel does have direct correlation with the output scale factor of the control system. There contains three important modules in the feedback channel of the accelerometer system: ① DA; ② VI converter; ③ Magnetic.

1) THE FIRST MODULE: k_{DA}

Similar to the analysis in the forward channel, the gain of the DA module can be computed as equation (9).

$$\begin{aligned}\hat{k}_{DA2} &= k_{DA2} \cdot (1 + \delta k_{DA2}) \\ &= \frac{V_{DA2\_ref}}{2^{N_{DA2}-1}} \cdot (1 + \delta V_{DA2\_ref}) \end{aligned} \tag{9}$$

2) THE SECOND MODULE: k_{VI}

The VI converter is composed of amplifier, resistance, etc. The theoretically expression of the gain of VI converter is stated in equation (10), and the most significant interfering factor is the drifting of sampling resistor.

$$k_{VI} = \frac{V_{in}}{R} \tag{10}$$

where V_{in} is the voltage from DA; R is the sampling resistor. The actual gain of the VI converter is $\hat{k}_{VI} = k_{VI} \cdot (1 + \delta k_{VI})$.

3) THE THIRD MODULE: $k_t = BL_{coil} \cdot L$

In the expression, L_{coil} is the length of coil winding; L is arm of ampere force. Both L_{coil} and L are the function of the

coefficient of linear expansion, and the actual expression of is stated in equation (11).

$$\hat{L}_{coil} \cdot \hat{L} = L_{c\&F} \cdot (1 + \delta L_{c\&F}) \tag{11}$$

B is the magnetic induction intensity of permanent magnet. In the quartz flexible accelerometer, only the magnetic vector parallel to coil plane could conclude effective electromagnetic force. Whereas the minor structural variation would change the direction of magnetic vector, resulting in the change of effective magnetic induction intensity. In addition, demagnetization, magnetic flux leakage could also affect the value of magnetic induction intensity. The effective value of B can be simplified as equation (12), considering all the influencing factors.

$$B_{real} = B \cdot (1 + \delta B) \tag{12}$$

Consequently, the gain of feedback could be computed as equation (13).

$$\begin{aligned}\hat{k}_{fb} &= k_{fb} \cdot (1 + \delta k_{fb}) \\ &= \frac{V_{DA2\_ref}}{2^{N_{DA2}-1}}(1 + \delta V_{DA2\_ref})k_{VI}(1 + \delta k_{VI}) \\ &\quad \cdot L_{c\&F}(1 + \delta L_{c\&F})B(1 + \delta B) \\ &= k_{fb} \cdot (1 + \delta V_{DA2\_ref})(1 + \delta k_{VI})(1 + \delta L_{c\&F})(1 + \delta B)\end{aligned} \tag{13}$$

III. THE ESTIMATION AND COMPENSATION METHOD OF THE LOOP-GAIN

A. THE ESTIMATION AND COMPENSATION OF THE FORWARD CHANNEL

As stated in chapter II, the gain variation is approximately linear changing. Rewrite the gain of forward channel:

$$\begin{aligned}\hat{k}_{pre} &= k_{pre} \cdot (1 + \delta k_{pre}) \\ &= \frac{1}{D} \cdot k_{demo}k(D(z)) \cdot \hat{k}_1 \cdot \hat{k}_{CV} \cdot \hat{k}_{AD}\end{aligned} \tag{14}$$

It can be conducted that $k(D(z))$ and $\hat{k}_1 \cdot \hat{k}_{CV} \cdot \hat{k}_{AD}$ do have identical effect on the overall gain. The variation of k_{pre}, if estimated, could be compensated in $k(D(z))$, which could be adjusted in FPGA. Then the performance of the close-loop controller would maintain the same with the initial condition.

The complete expression of the forward gain is stated in equation (15). And $\hat{k}_{pre}$ represents the relation between moment and the signal detection, as $N_{out} = \hat{k}_{pre} \cdot M_{in}$.

$$\begin{aligned}\hat{k}_{pre} &= k_{pre} \cdot (1 + \delta k_{pre}) \\ &= \frac{1}{D} \cdot k_{demo}k(D(z)) \cdot k_1(1 + \delta k_1) \cdot k_{CV}(1 + \delta k_{CV}) \\ &\quad \cdot k_{AD}(1 - \delta V_{AD\_ref}) \\ &= \frac{1}{D} \cdot k_{demo}k(D(z)) \cdot k_1(1 + \delta k_1) \\ &\quad \cdot N_{FPGA}k_{CV-T}(1 + \delta k_{CV}) \cdot k_{AD}(1 - \delta V_{AD\_ref})\end{aligned} \tag{15}$$

where k_{CV-T} is the gain of CV converter excluding N_{FPGA}. If the input moment, M_{in}, maintains constant, there can be conducted: $N_{out} \propto N_{FPGA}$. When the forward gain k_{pre} varies over time, the relation between N_{out} and N_{FPGA} does have the identical variation. Therefore, the estimation of the scale factor drifting between N_{out} and N_{FPGA} is the forward gain drifting, simultaneously.

When the quartz flexible accelerometer is in its open-loop state, the moving plate or the pendulum would be absorbed on the fixed plate, or the yoke iron. And the differential capacitance would be 0pF and $C_{\min}$, which maintains constant, shown in Fig. 4. The input moment maintains constant at this condition, and the output N_{out} is varied with N_{FPGA}.

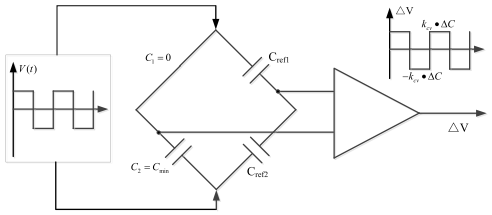

FIGURE 4. The transfer structure of the forward channel in open-loop state.

The circuit structure of the AC bridge is different from the close-loop state shown in Fig. 2. It is necessary to discuss the equivalence of the gain variation of AC bridge. The output of the instrument amplifier shown in Fig. 4. can be computed as equation (16). It indicates that there is just difference of the absolute value of gain, while the affection of the variation of C_{ref1}, C_{ref2} is identical with the normal AC bridge, relating to equation (5).

$$\Delta V = V_{IN} \cdot (1 - \frac{C_{ref1}}{C_{ref1} + C_{ref2}}) \cdot k_{amp} \tag{16}$$

Consequently, the estimation of the gain variation between N_{out} and N_{FPGA} could represent the variation of the forward gain in the open-loop state. In order to ensure the accuracy of measurement and inhibit the effect of random errors, there employs the least square method to estimate the gain variation, through changing the value of N_{FPGA}. The block diagram of the estimation schedule is shown in Fig. 5.

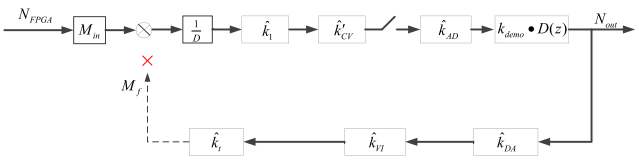

FIGURE 5. The block diagram of the estimation schedule.

The specific implementation steps are as follows.

1) In the initial status, the relation between N_{out} and N_{FPGA} is stated as follows:

$$N(i)_{out} = (N_{FPGA} + \Delta N(i)) \cdot k(D(z)) \cdot k_{pre-eq} \cdot M_{in} \tag{17}$$

where $\Delta N(i) = \{0, \Delta N_0, 2 \cdot \Delta N_0, \ldots n \cdot \Delta N_0\}$; $k_{pre-eq} = \frac{1}{D} \cdot k_{demo} \cdot k_1 \cdot k_{CV-T} \cdot k_{AD}$, and it do have

different absolute value but the same variation with the forward-gain, recorded as eq-forward-gain.

$$N(i)_{out} - N(0)_{out} = \Delta N(i) \cdot k(D(z)) \cdot k_{pre-eq} \cdot M_{in} \tag{18}$$

According to Least Square Criterion (19), shown at the bottom of this page.

2) In actual status, the relation between N_{out} and N_{FPGA} is stated in equation (20).

$$N(i)_{out} = (N_{FPGA} + \Delta N(i)) \cdot k(D(z)) \cdot k_{pre-eq} \cdot M_{in} \cdot (1 + \delta k_{pre}) \tag{20}$$

Similarly, $\Delta N(i) = \{0, \Delta N_0, 2 \cdot \Delta N_0, \ldots n \cdot \Delta N_0\}$.

$$N'(i)_{out} - N(0)_{out} = \Delta N(i) \cdot k(D(z)) \cdot k_{pre-eq}(1 + \delta k_{pre}) \cdot M_{in} \tag{21}$$

The gain variation $(1 + \delta k_{pre})$ could be conducted, relating to Least Square Criterion and the reference gain estimated in step 1).

3) The compensation of the gain variation can be conducted in the controller D(z), as shown in equation (22).

$$\begin{aligned} k(D(z)) \cdot k_{pre-eq} &= \left\{ \frac{1}{(1 + \delta k_{pre})} k(D(z)) \right\} \cdot k_{pre-eq}(1 + \delta k_{pre}) \\ &\approx \left\{ (1 - \delta k_{pre}) k(D(z)) \right\} \cdot k_{pre-eq}(1 + \delta k_{pre}) \end{aligned} \tag{22}$$

B. THE ESTIMATION AND COMPENSATION OF THE FEEDBACK CHANNEL

When the Digital-QFA is working in open-loop state, the output would be proportional to the excitation at the feedback-channel, shown in Fig. 6. and equation (23), where $a_{feedback}$ would balance the input acceleration. The entire loop-gain, $k_{pre} \cdot k_{fb}$, could be estimated through a_{in2} and N_{out}. Actually, when the Digital-QFA is at its open-loop state, it is unstable, and the electrostatic adsorption force would have great impact on the pendulum. Therefore, the testing repeatability could not achieve the precision for gain compensating.

$$N_{out} \propto a_{in2} \tag{23}$$

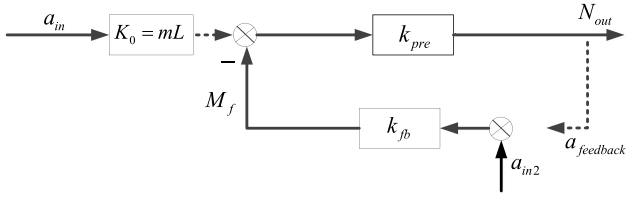

FIGURE 6. The open-loop model with additional acceleration excitation.

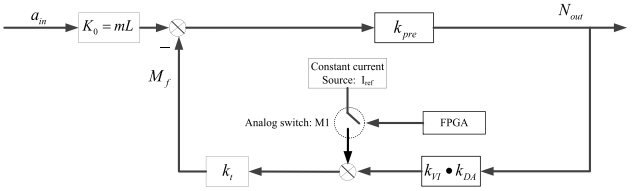

FIGURE 7. The close-loop model introduced with constant current source.

Through aging screening and temperature cyclic test, the variation of magnetic induction and the length of coil over time could be restrained at 5×10^{-6} per year, which means the transfer module k_t could be constant compared with the rest sections. The constant current source could achieve high precision, about 5×10^{-6} per year, and it is identical with the acceleration. Therefore, another acceleration reference, constant current source, could be introduced to the Digital-QFA, shown in Fig. 7. The analog switch M1 is controlled by FPGA, and it could be closed when conducting the estimation schedule, and it would be opened when in working-state, which do not impact the original close-loop working.

Therefore, the output of the entire close-loop system is stated in equation (24) and (25) separately when the switch on or off.

$$N_{out-on} = \frac{K_0 \cdot k_{pre}}{1 + k_{fb} \cdot k_{pre}} \cdot a_{in} + \frac{-k_t \cdot k_{pre}}{1 + k_t \cdot k_{VI} k_{DA} \cdot k_{pre}} \cdot I_{ref} \tag{24}$$

$$N_{out-off} = \frac{K_0 \cdot k_{pre}}{1 + k_{fb} \cdot k_{pre}} \cdot a_{in} \tag{25}$$

The loop-gain of the system would be much larger than 1, as $k_t \cdot k_{VI} k_{DA} \cdot k_{pre} \gg 1$. Then there can be concluded:

$$N_{out-on} - N_{out-off} \approx \frac{-1}{k_{VI} k_{DA}} \cdot I_{ref} \tag{26}$$

With the exact value of I_{ref}, the variation of could be estimated through N_{out-on} and $N_{out-off}$. And the practical operation steps are stated as follows:

1) In initial status, the relation between N_{out} and I_{ref}:

$$N_{out-on} - N_{out-off} \approx \frac{-1}{k_{VI} k_{DA}} \cdot I_{ref} \tag{27}$$

2) In actual status, the relation between N_{out} and I_{ref} is stated in equation (28).

$$N_{out-on} - N_{out-off} \approx \frac{-1}{k_{VI} k_{DA} \cdot (1 + \delta k_{fb})} \cdot I_{ref} \tag{28}$$

The gain variation $(1 + \delta k_{fb})$ would be computed, relating to the reference gain $k_{VI} k_{DA}$ in initial status, and the estimation error could be restrained in 10×10^{-6}.

$$k(D(z)) \cdot k_{pre-eq} \cdot M_{in} = \frac{\sum [(N(i)_{out} - N(0)_{out}) \Delta N(i)] - n \cdot \overline{(N(i)_{out} - N(0)_{out})} \cdot \overline{\Delta N(i)}}{\sum [\Delta N(i)]^2 - n \cdot (\overline{\Delta N(i)})^2} \tag{19}$$

3) Considering $(1 + \delta k_{fb})$ could only be compensated in the feedback channel, the compensation would be completed at the DA segment. The expression of the output of DA is stated in equation (29). Where N_{PI} is the result of the digital controller; N_{DA2} is the digits of DA; V_{DA2_ref} is the reference voltage of DA.

$$V_{DA2} = N_{PI} \cdot \frac{V_{DA2\_ref}}{2^{N_{DA2}-1}} \tag{29}$$

Actual, the reference voltage V_{DA2_ref} is provided through another DA, recorded as DA0. Therefore, the expression of V_{DA2_ref}, the output of DA0, is stated in equation (30). The variation of K_{DA0} is also embodied in $(1 + \delta k_{fb})$.

$$V_{DA2\_ref} = N_{VREF} \cdot K_{DA0} \tag{30}$$

where N_{VREF} is the digits transferring to DA0 from FPGA and it could be adjusted online. Consequently, the feedback gain variation could be compensated with $N'_{VREF} = N_{VREF} \cdot \frac{1}{(1+\delta k_{fb})} \approx N_{VREF} \cdot (1 - \delta k_{fb})$, controlled through FPGA. And the gain of feedback channel would be in consistent condition with the initial status.

In summary, the overall loop gain variation over time is compensated rationally through the separation of the gain of the forward and the feedback channel. The control structure diagram with compensation procession is shown in Fig. 8.

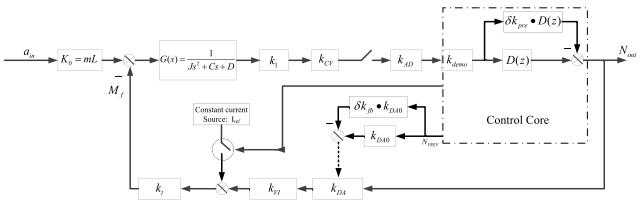

FIGURE 8. The control structure diagram with compensation procession.

IV. THE EXPERIMENTAL VERIFICATION OF THE COMPENSATION SCHEDULE

A. THE PROCEDURE OF EXPERIMENT

The compensation schedule is aiming at the gain variation over time. In order to simplify the test process, the loop-gain would be varied through changing the resistance value of the forward and feedback channel. And the absolute variation of the gain would be predictable and the estimation results could be judged precisely.

The estimation and compensation procedure are integrated in the accelerometer system, and the block diagram is presented in Fig. 9.

The testing procedure are conducted as follows:

1) At initial state, estimate the reference of the Eq-forward-gain and the entire-loop gain, recorded as $k_{pre-\mathrm{eq0}}$ and $k_{VI0}k_{DA0}$.
2) Fix the Digital-QFA in the stabilized platform, and conduct static testing. The average output of the accelerometer is recorded as $N_{out}(0)$.

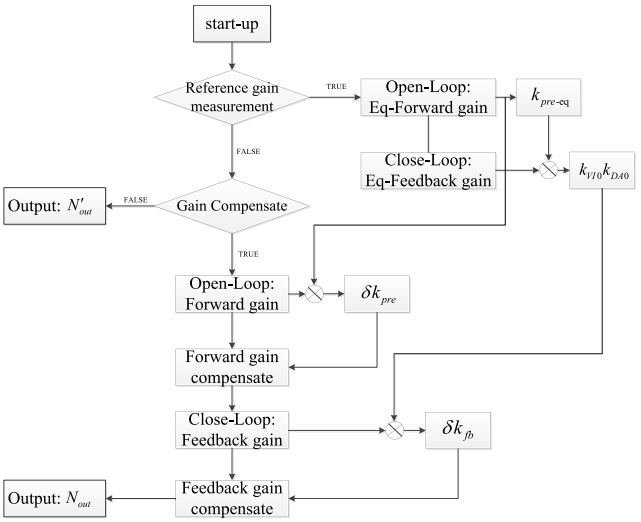

FIGURE 9. The estimation and compensation procedure.

3) Maintaining the install condition of accelerometer, the variation of the loop-gain is fixed to (−200ppm, +200ppm), separately for the forward and feedback channel. Conduct static testing without gain compensation. The average output of the accelerometer is recorded as N'_{out} (1).
4) Similar to step 3), conduct static testing after the compensation of loop gain. The average output of the accelerometer is recorded as N_{out} (1). And the new Eq-forward-gain, the gain of VI module and the DA module are recorded as $k_{pre-\mathrm{eq1}}$ and $k_{VI1}k_{DA1}$.
5) Execute comparative analysis with N_{out} (0), N'_{out} (1) and N_{out} (1).

B. THE RESULT OF ESTIMATION TEST

The estimation test is conducted as stated in section A. And the fundamental static performance indicators of Digital-QFA are shown in TABLE 2.

TABLE 2. The fundamental performance indicators of digital-QFA.

Performance	Quantity
Bias Stability	50ug
Bias Repeatability (one month)	50ug
Scale-Factor Linearity	30ppm
Scale-Factor Repeatability (one month)	30ppm

The structure and the circuit of the Digital-QFA tested are shown in Fig. 10.

1) THE ESTIMATION OF THE EQ-FORWARD-GAIN VARIATION

The estimation of the forward-gain is conducted with 6-times. The results are shown in TABLE 3, where $k_{pre\text{-eq0}}$ could be the benchmark value of the forward-gain, and $k_{pre\text{-eq1}}$

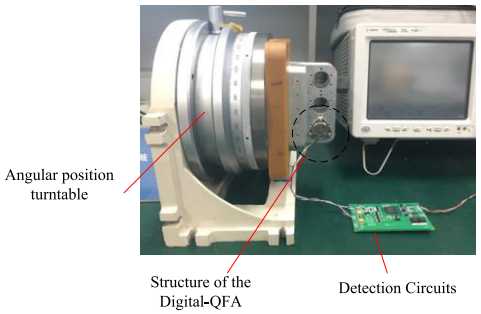

FIGURE 10. The structure and the circuit of the Digital-QFA.

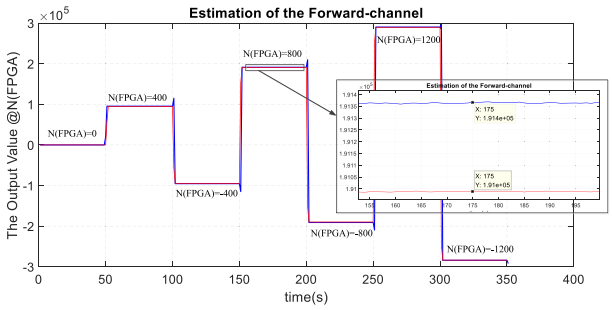

FIGURE 11. The Estimation of the Forward-gain drifting: (a) Blue line: the output value with no forward-gain error, $k_{pre\text{-}eq0}$; (b) Red line: the output value with forward-gain error (−200ppm), $k_{pre\text{-}eq1}$.

is the testing result of the real forward-gain when varying it by (-200ppm). Therefore, the relative variation between $(\frac{k_{pre\text{-}eq1}-k_{pre\text{-}eq0}}{k_{pre\text{-}eq0}} \cdot 10^6)(ppm)$ and $(-200ppm)$ could be the judgement of the effectiveness of the estimation procedure. As shown in TABLE 2, the estimated residuals of the procedure are about 9.74%, which means that about 90.26% of the error could be estimated and compensated.

TABLE 3. The estimation results of the Eq-forward-gain.

	$k_{pre\text{-}eq0}$	$k_{pre\text{-}eq1}$	$\delta k_{pre}=\frac{k_{pre\text{-}eq1}-k_{pre\text{-}eq0}}{k_{pre\text{-}eq0}}\bullet 10^6$ (ppm)	$\left\|\frac{\delta k_{pre}-(-200)}{-200}\right\|\bullet 100\%$
1	478.9735	478.8887	-177.04	11.48%
2	478.9761	478.8861	-187.90	6.05%
3	478.9697	478.8828	-181.43	9.28%
4	478.9771	478.8909	-179.96	10.02%
5	478.9706	478.8851	-178.50	10.75%
6	478.9764	478.8910	-178.29	10.85%
MEAN	**478.9739**	**478.8874**	**-180.53**	**9.74%**

One of the original data is shown in Fig. 11. , where (a) Blue-line: the Eq-forward-gain at initial status, or the reference forward-gain; (b) Red-line: the Eq-forward-gain when varying the forward parameter by (−200ppm).

2) THE ESTIMATION OF THE FEEDBACK-GAIN VARIATION

The estimation of the feedback-gain is also conducted with 6-times. The results are shown in TABLE 4, where $k_{VI0}k_{DA0}$

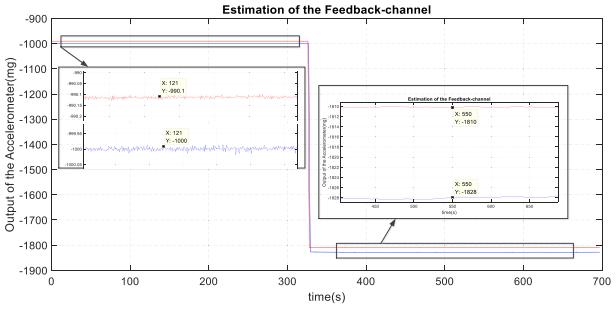

FIGURE 12. The Estimation of the Feedback-gain drifting: (a) Blue line: the output value with no feedback-gain error, $k_{VI0}k_{DA0}$; (b) Red line: the output value with feedback-gain error (+200ppm), $k_{VI1}k_{DA1}$.

could be the benchmark value of the feedback-gain, and $k_{VI1}k_{DA1}$ is the testing result of the real feedback-gain when varying it by (+200ppm). Therefore, the relative variation between $(\frac{k_{VI1}k_{DA1}-k_{VI0}k_{DA0}}{k_{VI0}k_{DA0}} \cdot 10^6)(ppm)$ and $(+200ppm)$ could be the judgement of the effectiveness of the estimation procedure. As shown in TABLE 3, the estimated residuals of the procedure are about 9.08%, which means that about 90.92% of the error could be estimated and compensated.

TABLE 4. The estimation results of the feedback-gain drifting.

	$k_{VI0}k_{DA0}$	$k_{VI1}k_{DA1}$	$\delta k_{fb}=(\frac{k_{VI1}k_{DA1}-k_{VI0}k_{DA0}}{k_{VI0}k_{DA0}}\bullet 10^6)$ (ppm)	$\left\|\frac{\delta k_{fb}-200}{+200}\right\|\bullet 100\%$
1	-71738.78	-71754.78	223.03	11.51%
2	-71738.14	-71753.42	212.99	6.50%
3	-71739.28	-71754.92	218.01	9.00%
4	-71739.21	-71754.63	214.94	7.47%
5	-71739.03	-71755.17	224.98	12.49%
6	-71738.67	-71754.09	214.94	7.47%
MEAN	**-71738.85**	**-71754.50**	**218.15**	**9.08%**

One of the original data is shown in Fig. 12., where (a) Blue-line: $k_{VI0}k_{DA0}$ at initial status, or the reference gain; (b) Red-line: $k_{VI1}k_{DA1}$ when varying the feedback parameter by (+200ppm). There are additional fluctuating errors when the constant current source be introduced to the system, and it does have strong correlation with the temperature. Also, the magnetic induction would be impacted by the temperature. These factors would degrade the estimation results, and enough testing time and stable environment temperature are necessary for high-precision estimation.

3) THE OUTPUT OF THE DIGITAL-QFA

One of the results of N_{out} (0), N'_{out} (1) and N_{out} (1) are integrated in Fig. 13 :

- The average of N_{out} (0) could be the accurate value of the accelerate;
- The average of N'_{out} (1) could be the output of the accelerometer without compensation;

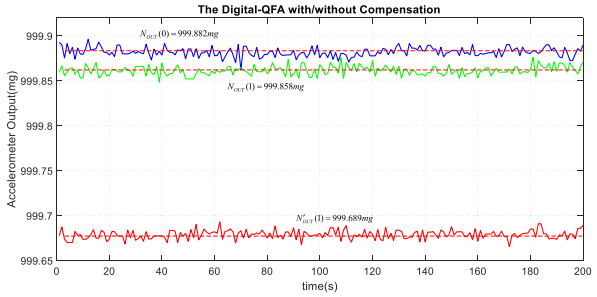

FIGURE 13. The output of the Digital-QFA with/without compensation: (a) Blue line: the output value with no loop-gain error, or the reference output; (b) Red line: the output value with loop-gain error and without compensation; (c) Green line: the output value with loop-gain error and with compensation.

- The average of N_{out} (1) could be the output of the accelerometer with compensation.

Without the gain compensation, there is difference 193ug between N_{out} (0) and N'_{out} (1), approximately. Through the online compensation of the loop gain, the difference between N_{out} (0) and N_{out} (1) is declined to 24ug, close to the static precision of the testing Digital-QFA. The estimation effect could be computed as equation (31).

$$\begin{aligned}\text{residual error} &= \frac{N'_{out}(1) - N_{out}(0)}{N_{out}(1) - N_{out}(0)} \times 100\% \\ &= \frac{24ug}{193ug} \times 100\% = 12.44\% \end{aligned} \tag{31}$$

The residual error of the estimation procedure is about 12.44%, which means that about 87.56% of the output error is restrained. The residual error would be the inaccurate measurement introduced by the magnetic induction, the length of the coil, etc. These factors were neglected rationally in the estimation model and the testing error is restrained in 10ppm.

There must be noticed that the entire testing procedure is conducted in laboratory and the fluctuation of room temperature is within 3°C. The large temperature fluctuation must be taken into consideration when applied in practical engineering, which could be calibrated in laboratory. Additionally, the estimation schedules are verified through changing the electrical parameters, and there are other elements which would vary over time. There should be more verification tests to check the effectiveness of the method, which would be the succeeding activities in our researches.

V. CONCLUSION

The entire model and the confounding factors in the Digital-QFA system over time are analyzed detailly. Most of the influence factors would bring about the variation of the loop gain, and ultimately, they would embody as the drifting of the output accelerate. Considering the gain of forward and feedback channel must be compensated separately, we propose two estimation schedules to distinguish the forward and the feedback gain variation, utilizing the modulating and the feedback signal. Through the simulation experiment, the estimation and compensation schedules are verified to be effective. And the testing results illustrate that about 87.56% of the variation of the output accelerate could be compensated. The long-term stability of the Digital-QFA would be promoted significantly.

Nevertheless, there still exist neglecting items in the compensation model, which lead to the residual of the compensation. And the long-term incentive mode is not identical with the temperature changing. To overcome this, we plan to establish more accurate models and pay more attention to the equivalence of the compensation mode and working mode. New detection circuits with equivalent topologies should also be included to the research content. Furthermore, long-term demonstration test is in progress to optimize the schedule.

REFERENCES

[1] J. H. van Nierop, "A low-cost linear accelerometer," *J. Phys. E, Sci. Instrum.*, vol. 14, no. 7, pp. 880–882, 1981.
[2] M. Chichinadze, V. Ilyin, A. Novgorodski, and N. Barbour, "Accelerometer designs and fields of application," in *Proc. 3rd Saint Petersburg Int. Conf. Integr. Navigat. Syst.*, 1996, pp. 115–125.
[3] W. Yang, B. Fang, Y. Y. Tang, and X. Qin, "A temperature compensation model for low cost quartz accelerometers and its application in tilt sensing," *Math. Problems Eng.*, vol. 2016, Aug. 2016, Art. no. 2950376.
[4] Z. Mohammed, G. Dushaq, M. Rasras, and A. Chatterjee, "An optimization technique for performance improvement of gap-changeable MEMS accelerometers," *Mechatronics*, vol. 54, pp. 203–216, Oct. 2018.
[5] J. He, W. Zhou, X. He, P. Peng, and H. Yu, "Structural designing of a MEMS capacitive accelerometer for low temperature coefficient and high linearity," *Sensors*, vol. 18, no. 2, p. 643, 2018.
[6] R. N. Dean, A. Anderson, S. J. Reeves, G. T. Flowers, and A. S. Hodel, "Electrical noise in MEMS capacitive elements resulting from environmental mechanical vibrations in harsh environments," *IEEE Trans. Ind. Electron.*, vol. 58, no. 7, pp. 2697–2705, Jul. 2011.
[7] *QA-2000 Accelerometer Data Sheet*, Honeywell Company, Charlotte, NC, USA, 2005.
[8] S. A. Foote and D. B. Grindeland, "Model QA3000 Q-flex accelerometer high performance test results," *IEEE Aerosp. Electron. Syst. Mag.*, vol. 7, no. 6, pp. 59–67, Jun. 1992.
[9] *Micro Electro Mechanical Systems (MEMS) on APC Market Study*, Syst. Planning Corp., Arlington County, VA, USA, 1994.
[10] N. Yazdi, F. Ayazi, and K. Najafi, "Micromachined inertial sensors," *Proc. IEEE*, vol. 86, no. 8, pp. 1640–1659, Aug. 1998.
[11] W. Yun, "A surface micromachined accelerometer with integrated CMOS detection circuitry," Ph.D. dissertation, Dept. Elect. Eng., Univ. California, Berkeley, San Francisco, CA, USA, 1992.
[12] B. E. Boser, "Design and implementation of oversampled analog-to-digital converters," Ph.D. dissertation, Dept. Elect. Eng., Stanford Univ., Palo Alto, CA, USA, 1988.
[13] R. C. Mehta, "Low-frequency sensitive force-balance linear standard accelerometer," *IEE Proc. A-Phys. Sci., Meas. Instrum., Manage. Educ.-Rev.*, vol. 134, pp. 45–57, Jan. 1987.
[14] C. Chen, M. Wu, Q. Wang, and J. Cao, "Analysis of stress on beam of small-range high-precision quartz flexible accelerometer," in *Proc. IEEE Int. Conf. Inf. Automat.*, Aug. 2015, pp. 2943–2946.
[15] C. Wang, X. Li, K. Kou, and C. Long, "Optimization of magnetic hat for quartz flexible accelerometer," *Sensor Rev.*, vol. 36, no. 1, pp. 71–76, 2016.
[16] Y. M. Wang, P. K. Chan, H. K. H. Li, and S.-E. Ong, "A low-power highly sensitive capacitive accelerometer IC using auto-zero time-multiplexed differential technique," *IEEE Sensors J.*, vol. 15, no. 11, pp. 6179–6191, Nov. 2015.
[17] M. A. Lemkin, M. A. Ortiz, N. Wongkomet, B. E. Boser, and J. H. Smith, "A 3-axis surface micromachined ΣΔ accelerometer," in *IEEE Int. Solid-State Circuits Conf. (ISSCC) Dig. Tech. Papers*, Feb. 1997, pp. 202–203.
[18] P. K. Chan and J. Cui, "Design of chopper-stabilized amplifiers with reduced offset for sensor applications," *IEEE Sensors J.*, vol. 8, no. 12, pp. 1968–1980, Dec. 2008.

[19] W. F. Lee and P. K. Chan, "A capacitive-based accelerometer IC using injection-nulling switch technique," *IEEE Trans. Circuits Syst. I, Reg. Papers*, vol. 55, no. 4, pp. 980–989, May 2008.
[20] I. Saied and M. Meribout, "Electronic hardware design of electrical capacitance tomography systems," *Phil. Trans. Roy. Soc. A, Math., Phys. Eng. Sci.*, vol. 374, no. 2070, 2016, Art. no. 20150331.
[21] W. Q. Yang and T. A. York, "New AC-based capacitance tomography system," *IEE Proc.-Sci., Meas. Technol.*, vol. 146, no. 1, pp. 47–53, Jan. 1999.
[22] W. Q. Yang, A. L. Stott, and J. C. Gamio, "Analysis of the effect of stray capacitance on an ac-based capacitance tomography transducer," *IEEE Trans. Instrum. Meas.*, vol. 52, no. 5, pp. 1674–1681, Oct. 2003.
[23] J. Szabatin, V. E. Melnikov, and A. A. Platonov, "Analog-digital wide-range measurement systems with adaptively adjusted quartz glass sensors," in *Proc. IEEE Instrum. Meas. Technol. Conf.*, Jun. 1996, pp. 1154–1159.
[24] P. Eykhoff, *System Identification Parameter and State Estimation*. Hoboken, NJ, USA: Wiley, 1974.
[25] R. Isermann and M. Münchhof, *Identification of Dynamic Systems: An Introduction With Applications*. Berlin, Germany: Springer-Verlag, 2011.
[26] T. Luspay, B. Kulcsar, J.-W. van Wingerden, M. Verhaegen, and J. Bokor, "Linear parameter varying identification of freeway traffic models," *IEEE Trans. Control Syst. Technol.*, vol. 19, no. 1, pp. 31–45, Jan. 2011.
[27] S.-B. Lee, "Closed-loop estimation of permanent magnet synchronous motor parameters by PI controller gain tuning," *IEEE Trans. Energy Convers.*, vol. 21, no. 4, pp. 863–870, Dec. 2006.
[28] S.-H. P. Won and F. Golnaraghi, "A triaxial accelerometer calibration method using a mathematical model," *IEEE Trans. Instrum. Meas.*, vol. 59, no. 8, pp. 2144–2153, Sep. 2010.
[29] P. Batista, C. Silvestre, P. Oliveira, and B. Cardeira, "Accelerometer calibration and dynamic bias and gravity estimation: Analysis, design, and experimental evaluation," *IEEE Trans. Control Syst. Technol.*, vol. 19, no. 5, pp. 1128–1137, Sep. 2011.
[30] P. Gao, K. Li, L. Wang, and Z. Liu, "A self-calibration method for accelerometer nonlinearity errors in triaxis rotational inertial navigation system," *IEEE Trans. Instrum. Meas.*, vol. 66, no. 2, pp. 243–253, Feb. 2017.
[31] L. Wang, W. Wang, Q. Zhang, and P. Gao, "Self-calibration method based on navigation in high-precision inertial navigation system with fiber optic gyro," *Opt. Eng.*, vol. 53, no. 6, Jun. 2014, Art. no. 064103.
[32] S. Yusheng, D. Lianjin, and Y. Kui, "Parameter calculation and error term analysis of quartz flexible accelerometer," (in Chinese), *J. Vib., Meas. Diagnosis*, vol. 5, no. 3, pp. 13–22, 1984.

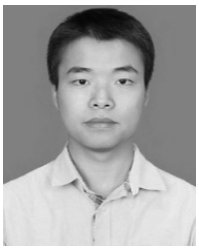

LONGJUN RAN was born in 1991. He is currently pursuing the Ph.D. degree with the School of Instrumentation Science and Opto-electronics Engineering, Beihang University. His research interests include redundant SINS technique, integrated SINS/GPS/Odometer technique, the digital close-loop accelerometer, and modern control systems.

CHUNXI ZHANG was born in 1965. He is currently pursuing the Ph.D. degree with the School of Instrumentation Science and Opto-electronics Engineering, Beihang University, where he is also a Professor. His research interests include fiber optical gyroscopes technique, GPS/SINS integrated navigation technique, photoelectric detecting, and signal processing technique.

LAILIANG SONG received the Ph.D. degree from the School of Instrumentation Science and Opto-electronics Engineering, Beihang University, Beijing, China, in 2014, where he has been an Instructor, since 2014. His current research interests include the redundant SINS technique, integrated GPS/SINS technique, FDI technique, and digital closed-loop accelerometer.

JIAZHEN LU was born in 1982. He received the Ph.D. degree from the School of Instrumentation Science and Opto-electronics Engineering, Beihang University, Beijing, China, in 2009, where he was a Lecturer, from 2009 to 2019. He is currently a Professor with the School of Aeronautics and Astronautics, Central South University, Changsha, China. His current research interests include integrated navigation and control engineering.